Inference of Vehicle Lane Change Intention Using Multiple Model Estimator in Automated Highway Driving

Jongyong Do[1], Kyoungseok Han[2], and Seibum B. Choi[1]*

[1]Department of Mechanical Engineering, Korea Advanced Institute of Science and Technology,
Daejeon, 34141, Korea (djy0129@kaist.ac.kr, sbchoi@kaist.ac.kr) * Corresponding author
[2]Department of Mechanical Engineering, Kyungpook National University,
Daegu, 41566, Korea (kyoungsh@knu.ac.kr)

Abstract: One of the most critical topics in vehicle active safety control is collision avoidance(CA) maneuver. To ensure the robustness of the CA, it is essential to recognize the behavior of surrounding vehicles accurately. In particular, a safer path can be generated, if the intention of changing lanes of surrounding vehicles can be predicted. Existing studies on lane change intention prediction are primarily based on machine learning, and it is difficult to respond to unexpected situations that have not been learned. In this study, a method for predicting lane change intention in real time based on the trajectory of surrounding vehicles is presented. It is assumed that the location of the lane is known through the map, and the global coordinate system is transformed into the Frenet coordinate system to maintain generality regardless of the curvature of the road. And the paths that the target vehicle can travel are modeled as cubic spline curves on the Frenet coordinate system. Through the multiple model estimator, which operates the path models in parallel, it finds the most probable path and predicts the lane change intention. The performance of the lane change intention prediction algorithm is verified through highD, a German highway vehicle trajectories dataset.

Keywords: Lane-change intention, Multiple model estimator, Unscented Kalman filter, Cubic spline, Frenet coordinates

1. INTRODUCTION

As the level of Advanced Driver Assistance Systems (ADAS) increases, so does active safety control performance. Research to ensure high reliability of vehicle safety by using V2X technology that can know the information of nearby vehicles and traffic infrastructure through communication is also being actively conducted. Also, high-definition maps are being built over a broader range. Due to this background, autonomous vehicles can more accurately perceive their surroundings through a large amount of information and perform active safety control [1]. In order to perform control, a decision must be made based on the perception result.

Lane change decision-making of the ego vehicle is a very complex problem, and various studies have been conducted on this. First, there is a method to analyze model probability by designing an Interacting Multiple Model estimator based on the Lane change model [2]. Most of the existing studies are data-based learning, and typically support vector machine (SVM) [3] and deep reinforcement learning (Deep RL) [4], [5] are applied. And recently, researches using game theory have also been conducted [6], [7]. If there is an error in the autonomous vehicle's lane change decision-making on the highway, there is a high possibility of a serious accident. If the ego vehicle can recognize the lane change intention of the surrounding vehicle, it can make a more accurate decision. Most existing studies on lane change intention prediction of surrounding vehicles also use learning [8]. There are many studies such as SVM and Neural Networks (NN) [9], Long short-term memory (LSTM) [10], [11], and Fuzzy logic with NN [12]. And recently, there have been attempts to build a Human-like Lane Changing

Intention Understanding Model (HLCIUM) [13].

Lane changing intention prediction is influenced by many factors such as driver's disposition and surrounding traffic conditions, so it is impossible to model it considering all situations, and it relies heavily on data. However, the data-driven learning method does not respond to real-time emergencies, and it is difficult to determine the cause when making a wrong decision. In this study, an algorithm that can determine the intention to change lanes in real time based on the trajectories of surrounding vehicles without relying on big data is proposed.

2. COORDINATE TRANSFORMATION AND PATH MODELING

In this study, it is assumed that lane locations are known through maps. In other words, the global(Cartesian) coordinates of the lane are known, and the global coordinate system is transformed into the Frenet coordinate system to maintain generality regardless of road curvature. After that, the paths that the target vehicle can travel are modeled in the form of cubic spline curves in the Frenet coordinate system.

2.1 Frenet coordinate system

If the global coordinates of the lane are known, it is possible to estimate the coordinates that the target vehicle will follow when maintaining or changing lanes at the current location. Also, the coordinates that the target vehicle is expected to follow can be expressed as a function of the global coordinate system. This is similar to predicting the trajectory of a target vehicle when a human is driving. However, if this process is carried out in the global coordinate system, the shape of the function does

not appear consistently depending on the curvature of the road. If it is a straight road without any curvature, a path can be generated in a consistent form from the current location of the target vehicle. However, if there is curvature, the shape of the path is distorted according to the direction in which the target vehicle is moving. Therefore, in order to ensure generality so that it can be applied to all roads, curvature roads should be transformed into straight roads. Such a curvilinear coordinate system is called a Frenet coordinate system. Fig. 1 and Fig. 2 shows the transformation process from the global coordinate system to the Frenet coordinate system [14].
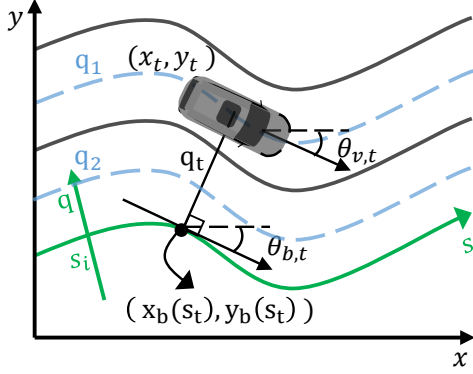
Fig. 1. Global coordinate system and base frame.
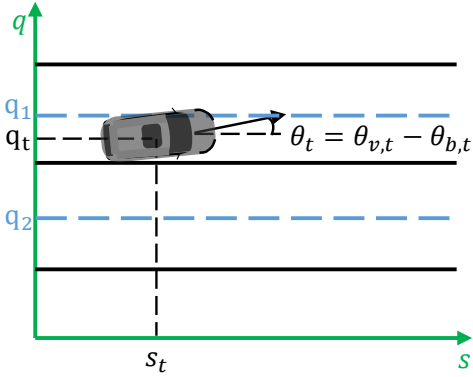
Fig. 2. Frenet coordinate system.

Fig. 1 represents a curvature road in the global x-y coordinate system, and the current location of the target vehicle is at (x_t, y_t). Since the global coordinates of the lanes are known, the position of the target vehicle is indicated with respect to one of the lanes. The standard line is the base frame, and the length of this line is s. The vertical distance away from the base frame is q. From the vehicle's point of view, s is the longitudinal travel distance of the vehicle, and q is the lateral offset from the base frame. The base frame is represented by parameterizing x and y in the global coordinate system as a cubic function for s, respectively, in Eqs. (1)~(2).

$$x_b(s) = a_{x,i}(s - s_i)^3 + b_{x,i}(s - s_i)^2 + c_{x,i}(s - s_i) + d_{x,i}, \tag{1}$$

$$y_b(s) = a_{y,i}(s - s_i)^3 + b_{y,i}(s - s_i)^2 + c_{y,i}(s - s_i) + d_{y,i}. \tag{2}$$

$a_{x,i}, b_{x,i}, c_{x,i}, d_{x,i}$ are coefficients of the cubic spline curve of x with respect to s, and y is the same expression. When the coordinates x_b and y_b of the base frame are expressed as a parametric curve for s, sections are divided by s range and coefficients for each section are obtained. s_i is the s value at the initial position of the ith section. The reason for dividing the section is to accurately express a point on the base frame as a spline curve for s. If the points on the long base frame are expressed as a single spline curve, the error between the actual points and the curve increases. However, if the section is subdivided too much, the amount of calculation is increased, so the length of the section must be appropriately adjusted. It may be possible to change the length of the section according to the curvature. In Fig. 1, $\theta_{v,t}$ and $\theta_{b,t}$ for the current position of the target vehicle represent the heading angle and the instantaneous inclination in the base frame in the global coordinate system, respectively Eqs. (3)~(4).

$$\tan \theta_v = \frac{V_y}{V_x}, \tag{3}$$

$$\tan \theta_b = \frac{\frac{dy}{ds}}{\frac{dx}{ds}}. \tag{4}$$

It is assumed that the x and y coordinates of the target vehicle and the velocities V_x and V_y in the x and y directions in the global coordinate system can be measured through a sensor in the ego vehicle or can be known through communication between vehicles. Then, s can be obtained through the x and y coordinates, and the slope of the base frame with respect to this s can also be obtained. The distance from the base frame to the target vehicle is calculated numerically by Newton's method [15]. After all, the situation in the global coordinate system of Fig. 1 can be expressed in the Frenet coordinate system as in Fig. 2. In the Frenet coordinate system, the current position of the target vehicle is indicated by s_t and q_t, and the heading angle is θ_t. θ is the difference between the heading angle of the vehicle and the angle with respect to the instantaneous inclination in the base frame, as shown in Eq. (5).

$$\theta = \theta_v - \theta_b. \tag{5}$$

2.2 Path modeling

After transforming the global coordinate system into the Frenet coordinate system, model the path that the target vehicle can go. For example, when there are lanes on

either side of the lane where the target vehicle is driving, the vehicle maneuvers in one of three cases: lane change to the left, lane keeping, and lane change to the right. It can be modeled in the form of a cubic spline curve. Fig. 3 describes the above.
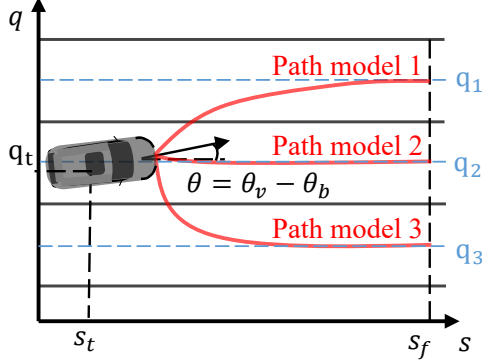
Fig. 3. Path models in the form of cubic spline curves in Frenet coordinates.

In the Frenet coordinate system, the current position of the target vehicle is (s_t, q_t) and the heading angle is θ. q_1, q_2, and q_3 are q values of lane centers to which the target vehicle can go. The path model expression can be expressed as Eq. (6).

$$q = a(s - s_t)^3 + b(s - s_t)^2 + c(s - s_t) + d. \\ (s_t \leq s \leq s_f) \qquad (6)$$

a, b, c, and d are the coefficients of the cubic spline curve, which can be determined by four boundary conditions for the initial and final points of the path as shown in Eq. (7).

$$1) q(s_t) = q_t \qquad 2) \frac{dq}{ds}(s_t) = \tan\theta_v - \theta_b$$
$$3) q(s_f) = q_i + \Delta q \qquad 4) \frac{dq}{ds}(s_f) = 0. \qquad (7)$$
$$(\Delta q = -4, 0, 4)$$

Conditions 1) and 2) relate to path initial coordinates and heading angle, and conditions 3) and 4) relate to path final coordinates and heading angle. q_i is the distance from the base frame to the current lane center of the target vehicle. Δq is set to 4 when changing lane in the direction away from the base frame, -4 when changing lane in the direction closer to the base frame, and 0 when keeping the lane. The path final point, s_f, is set variably according to the speed of the vehicle and can be expressed as Eq. (8).

$$s_f = V_t t_{prev} + s_t. \qquad (8)$$

s_t is the current position of the target vehicle and V_t is the speed. t_{prev} is the preview time and means the time it takes to change lane. $s_f - s_t$ is the distance traveled

until the lane change is completed. The result of calculating the coefficients of the cubic spline curve by applying boundary conditions is Eq. (9).

$$\begin{bmatrix} a \\ b \end{bmatrix} =$$
$$\begin{bmatrix} (s_f - s_t)^3 & (s_f - s_t)^2 \\ 3(s_f - s_t)^2 & 2(s_f - s_t) \end{bmatrix}^{-1} \begin{bmatrix} q_i + \Delta q - q_t - c(s_f - s_t) \\ -c \end{bmatrix}$$
$$c = tan(\theta_v - \theta_b), \quad d = q_t. \qquad (9)$$

The lane change intention of the target vehicle is estimated using the path model.

3. LANE CHANGE INTENTION INFERENCE

Since the cubic spline path model in Chapter 2 has nonlinearity, it is not possible to use the Kalman filter applicable only to the linear model. Therefore, an extended Kalman filter(EKF) that linearizes a nonlinear function or an unscented Kalman filter(UKF) that uses a probabilistic method through several samples can be considered. Since it is generally known that the performance of EKF cannot be guaranteed when the order is more than the 3rd order, the UKF is used in this study. When there are several lanes that the target vehicle can go from the current location, a multiple model estimator that uses path models in parallel is configured. Multiple model-based adaptive estimator applies the UKF to each path model to find likelihood and update mode probability and posterior. At this time, it determines which path is most likely to go through the mode probability and determines the intention to change lanes.

3.1 Unscented Kalman filter using path model

The states of the nonlinear model are set as s and q in the Frenet coordinate system, and the state vector is expressed as X. Measurements are x and y in the global coordinate system, and the measurement vector is denoted by Y. In the discrete-time domain, the state space form can be expressed as follows.(Eqs. 10~11)

$$X_k = \begin{bmatrix} s_k \\ q_k \end{bmatrix} = f(X_{k-1}) + w_k,$$
$$f(X_{k-1}) = \begin{bmatrix} V_{k-1}dt + s_{k-1} \\ a(V_{k-1}dt)^3 + b(V_{k-1}dt)^2 + c(V_{k-1}dt) + q_{k-1} \end{bmatrix}. \qquad (10)$$

$$Y_k = \begin{bmatrix} x_k \\ y_k \end{bmatrix} = h(X_k) + v_k,$$
$$h(X_k) = \begin{bmatrix} x_b(s_k) - q_k \sin\theta_b \\ y_b(s_k) + q_k \cos\theta_b \end{bmatrix}. \qquad (11)$$

In the above nonlinear dynamic system, w_k means model uncertainty and v_k means measurement noise, and both terms are the additive white Gaussian noise. s_k is obtained by adding s_{k-1} to the value multiplied by the speed V_{k-1} and the sampling time dt. The q_k of

the kth step is obtained from the path model created in the $(k-1)^{th}$ step. The measurement model means that (s_k, q_k) of the Frenet coordinate system is transformed back into the global coordinate system (x_k, y_k). In the UKF, estimation is performed by comparing the global coordinates of the target vehicle measured by the sensor with the value calculated by the measurement model. The UKF application process is as follows [16], [17], [18].

1) Initialization:

$$\hat{X}_0^+ = E(X_0), \quad \hat{P}_0^+ = E\left[(X_0 - \hat{X}_0^+)(X_0 - \hat{X}_0^+)^T\right]. \quad (12)$$

2) State prediction:
2-1) Sigma points for posterior distribution.

$$\hat{X}_{k-1}^{(i)} = \hat{X}_{k-1}^+ + \left(\sqrt{nP_{k-1}^+}\right)_i^T, \quad i = 1, \cdots, n, \quad (13a)$$

$$\hat{X}_{k-1}^{(i)} = \hat{X}_{k-1}^+ - \left(\sqrt{nP_{k-1}^+}\right)_{i-n}^T, \quad i = n+1, \cdots, 2n. \quad (13b)$$

2-2) Propagate the sigma points with $f(X)$.

$$\hat{X}_k^{(i)} = f\left(\hat{X}_{k-1}^{(i)}\right). \quad (14)$$

2-3) Prior state estimate and covariance.

$$\hat{X}_k^- = \frac{1}{2n}\sum_{i=1}^{2n}\hat{X}_k^{(i)}, \quad (15a)$$

$$P_k^- = \frac{1}{2n}\sum_{i=1}^{2n}\left(\hat{X}_k^{(i)} - \hat{X}_k^-\right)\left(\hat{X}_k^{(i)} - \hat{X}_k^-\right)^T + Q_{k-1}. \quad (15b)$$

Where Q_{k-1} is the process noise covariance.

3) Measurement prediction:
3-1) Sigma points for prior distribution.

$$\hat{X}_k'^{(i)} = \hat{X}_k^- + \left(\sqrt{nP_k^-}\right)_i^T, \quad i = 1, \cdots, n, \quad (16a)$$

$$\hat{X}_k'^{(i)} = \hat{X}_k^- - \left(\sqrt{nP_k^-}\right)_{i-n}^T, \quad i = n+1, \cdots, 2n. \quad (16b)$$

3-2) Sigma points update with $h(X)$.

$$\hat{Y}_k^{(i)} = h\left(\hat{X}_k'^{(i)}\right). \quad (17)$$

3-3) Predicted measurement and covariance.

$$\hat{Y}_k = \frac{1}{2n}\sum_{i=1}^{2n}\hat{Y}_k^{(i)}, \quad (18a)$$

$$P_Y = \frac{1}{2n}\sum_{i=1}^{2n}\left(\hat{Y}_k^{(i)} - \hat{Y}_k\right)\left(\hat{Y}_k^{(i)} - \hat{Y}_k\right)^T + R_k. \quad (18b)$$

Where R_k is the measurement noise covariance.

4) Measurement update:

4-1) The cross covariance between $\hat{x}_k^-$ and $\hat{y}_k$.

$$P_{XY} = \frac{1}{2n}\sum_{i=1}^{2n}\left(\hat{X}_k^{(i)} - \hat{X}_k^-\right)\left(\hat{Y}_k^{(i)} - \hat{Y}_k\right)^T. \quad (19)$$

4-2) Kalman gain.

$$K_k = P_{XY}P_Y^{-1}. \quad (20)$$

4-3) Posterior state estimate and error covariance.

$$\hat{X}_k^+ = \hat{X}_k^- + K_k\left(Y_k - \hat{Y}_k\right), \quad (21a)$$

$$P_k^+ = P_k^- - K_k P_Y K_k^T. \quad (21b)$$

3.2 Multiple model estimator design

The UKF is applied to each of the path models that the target vehicle is expected to follow in the future. The likelihood is calculated by comparing the coordinates predicted through the model and the measured coordinates, and the probability of each model is calculated. The transition between each lane model is not considered, so a static multiple model estimator(SMM) is used. These processes are shown in Fig. 4.
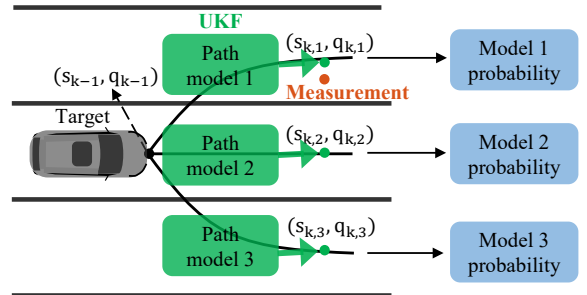
Fig. 4. Scheme of the lane change intention prediction.

The paths that the target vehicle can travel are modeled as cubic spline curves, and the next step positions are predicted through these path models. Then, the mode probabilities representing the probabilities of going to each path are calculated by comparing the measurements and the predictions of each model. Through these mode probabilities, it is possible to determine the lane change intention of the target vehicle. For example, in Fig.4, if the probability for path model 1 is the highest, it is determined that the vehicle intends to change lane to the left. It can be interpreted that the closer the probability of path model 1 is to 1, the clearer the intention to change the lane to the left. In SMM, the mode probability is calculated using the likelihood function as shown in Eq. (22) [16].

$$p(r_k|m = i) = \frac{exp\left(-0.5 r_k^T[i] S_k^{-1}[i] r_k[i]\right)}{\sqrt{(2\pi)^n |S_k[i]|}}. \quad (22)$$

$r_k[i]$ is the innovation that is the difference between measurement and model value in the ith mode, and $S_k[i]$ is the covariance of the innovation in the ith mode. The mode probability is obtained through likelihood Eq. (23).

$$\alpha_k[i] = \frac{\alpha_{k-1}[i] \cdot p(r_k|m = i)}{\sum\limits_{j=1}^{M} \alpha_{k-1}[j] \cdot p(r_k|m = j)}. \tag{23}$$

The ith mode probability is obtained using the ith mode probability at the $(k-1)^{th}$ step and the likelihood at the kth step. The overall flow of SMM is shown in Fig. 5.
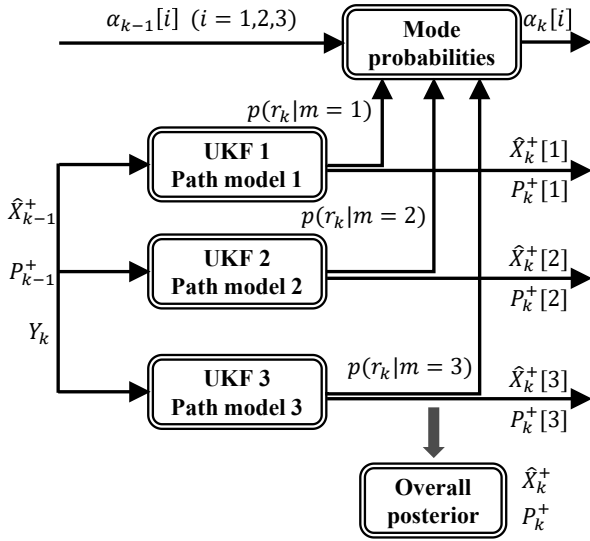
Fig. 5. Structure of static multiple model estimator.

P_k is the error covariance. For each step, the final posterior and error covariance are obtained by multiplying the mode probability by the weight of each mode posterior and error covariance. (Eq. (24))

$$\hat{X}_k^+ = \sum_{i=1}^{M} \alpha_k[i] \hat{X}_k^+[i], \tag{24a}$$

$$P_k^+ = \sum_{i=1}^{M} \alpha_k[i] \left[P_k^+[i] + \left(\hat{X}_k^+[i] - \hat{X}_k^+ \right) \left(\hat{X}_k^+[i] - \hat{X}_k^+ \right)^T \right]. \tag{24b}$$

3.1 UKF and 3.2 SMM are repeated every step to estimate lane change intention.

4. TEST RESULTS

Chapters 2 to 3 presented SMM that calculates the probability for each model by applying UKF to the path models. Chapter 4 is about the performance verification of the SMM algorithm that estimates the lane change intention of the target vehicle using highD [19]. The

highD is a vehicle trajectories dataset on German highways that records the driving trajectories of real vehicles with drones. Various situations including lane change are recorded in highD, and the accuracy is high with a typical positioning error of less than 10cm. Since lane change is also recorded in the dataset, the algorithm is applied and verified on vehicle data that changes lane. The width of the lane is fixed at 4 m. The vehicle data used for verification is shown in Fig. 6.
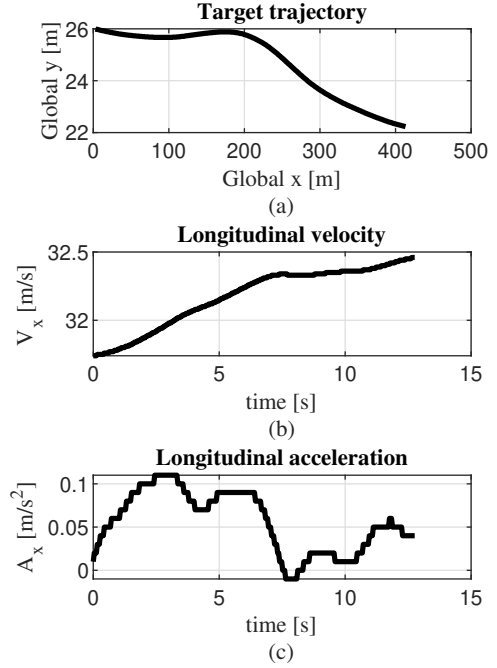
Fig. 6. Vehicle data: (a) trajectory; (b) longitudinal velocity; (c) longitudinal acceleration

As already mentioned, the coordinates of the lanes are known from the map. The SMM algorithm is applied to determine the intention to change lanes, considering that the position and speed of the target vehicle can be measured. The vehicle data is visualized in Matlab to verify the algorithm, and some of the results are shown in Fig. 7~9. In all three cases, lanes and target vehicles are displayed in the Frenet coordinate system. The left lane changing path is shown in blue, the lane keeping path is shown in red, and the right lane changing path is shown in yellow. In SMM, the path with high probability appears thicker. This means that the thicker the path, the higher the probability of going to that path.

Fig. 7 is a situation in which the probability of the vehicle keeping the lane is about 0.6, and the probability of changing the lane to the right (the direction in which q is lowered) is about 0.4. Since there is no lane to the left of the target vehicle, the probability for this is zero. In Fig. 8, the probability of changing lanes to the right becomes 1, so that the thickness of the yellow path is maximum. Finally, Fig. 9 shows that the probability of keeping the lane is 1 because the vehicle has completed the lane change. Fig. 10 shows the trajectory of the tar-
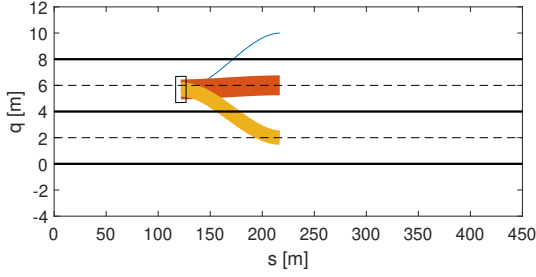
Fig. 7. Simulation result using highD (lane change intention detection).
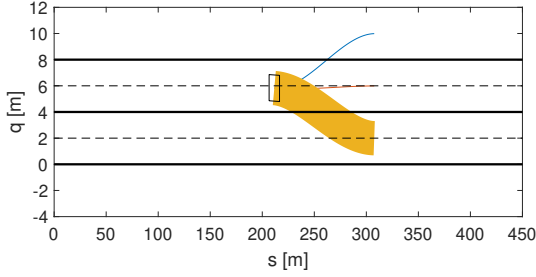
Fig. 8. Simulation result using highD (lane changing).
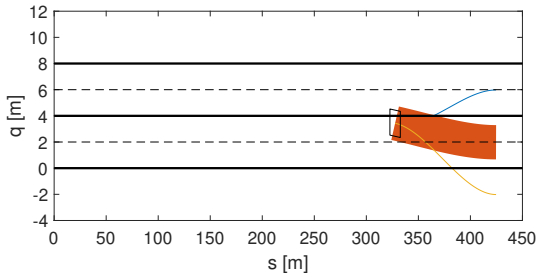
Fig. 9. Simulation result using highD (lane keeping).

get vehicle in the Frenet coordinate system, and Fig. 11 shows the path model probabilities corresponding to s.

Comparing and analyzing Fig.10 and Fig.11, it can be concluded that the algorithm reflects the intention of the vehicle well. When s is within $100m$, the lane change intention probability is about 0.4 as the vehicle moves in the direction where q decreases. When s exceeds $100m$, the lane change probability exceeds 0.8 instantaneously, but the lane keeping probability becomes one as q increases again. It can be seen that when s is about $200m$, the lane change probability becomes one as the curvature increases in the direction in which q decreases.

5. CONCLUSION

In autonomous driving, decision-making is a crucial step directly related to safety, but due to the high complexity, it is sometimes difficult to consider all situations well. In the case of automated highway driving, lane change decision-making errors are fatal. If the lane change intentions of surrounding vehicles can be predicted, these errors can be reduced. In this study, the lane change intention of surrounding vehicles is predicted
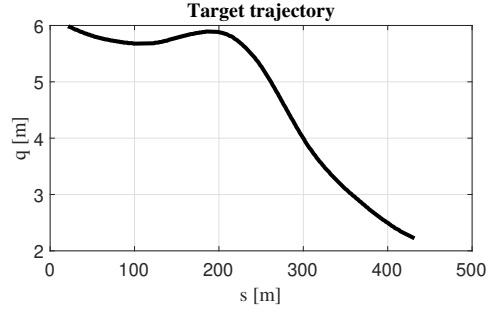
Fig. 10. Trajectory of the target vehicle in the Frenet coordinate system.
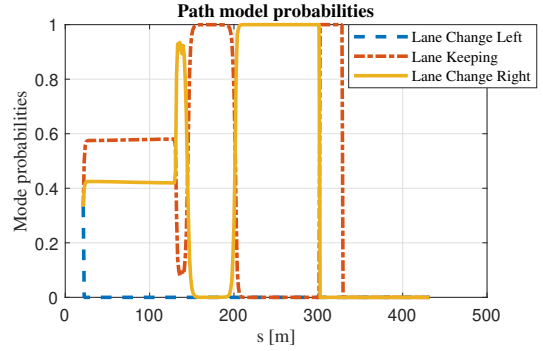
Fig. 11. Path model probabilities calculated by SMM.

using the path model. Path modeling is done by transforming the global coordinate system to the Frenet coordinate system so that it can be generally applied to all roads. After that, UKF is designed using the path model, and the multiple model estimator is constructed using the path models in parallel. Estimator performance is verified through highD.

In this study, the preview time is set as a tuning parameter, but in the future, preview time adaptation using the past trajectory will be performed. Furthermore, the trajectory expected to follow when changing lanes can be predicted using the preview time for each lane.

REFERENCES

[1] Han, Kyoungseok, et al. "Model predictive control framework for improving vehicle cornering performance using handling characteristics." *IEEE Transactions on Intelligent Transportation Systems* 22.5 (2020): 3014-3024.

[2] Liu, Jiang, et al. "GNSS/INS-based vehicle lane-change estimation using IMM and lane-level road map." *16th International IEEE Conference on Intelligent Transportation Systems (ITSC 2013)*. IEEE, 2013.

[3] Liu, Yonggang, et al. "A novel lane change decision-making model of autonomous vehicle based on support vector machine." *IEEE access* 7 (2019): 26543-26550.

[4] Alizadeh, Ali, et al. "Automated lane change decision making using deep reinforcement learning in dynamic and uncertain highway environment." *2019 IEEE intelligent transportation systems conference (ITSC)*. IEEE, 2019.

[5] Wang, Junjie, et al. "Lane change decision-making through deep reinforcement learning with rule-based constraints." *2019 International Joint Conference on Neural Networks (IJCNN)*. IEEE, 2019.

[6] Hang, Peng, et al. "Human-like decision making for autonomous driving: A noncooperative game theoretic approach." *IEEE Transactions on Intelligent Transportation Systems* 22.4 (2020): 2076-2087.

[7] Lopez, Victor G., et al. "Game-theoretic lane-changing decision making and payoff learning for autonomous vehicles." *IEEE Transactions on Vehicular Technology* 71.4 (2022): 3609-3620.

[8] Song, Ruitao, and Bin Li. "Surrounding vehicles' lane change maneuver prediction and detection for intelligent vehicles: A comprehensive review." *IEEE Transactions on Intelligent Transportation Systems* (2021).

[9] Benterki, Abdelmoudjib, et al. "Prediction of surrounding vehicles lane change intention using machine learning." *2019 10th IEEE International Conference on Intelligent Data Acquisition and Advanced Computing Systems: Technology and Applications (IDAACS)*. Vol. 2. IEEE, 2019.

[10] Han, Teawon, Junbo Jing, and Ümit Özgüner. "Driving intention recognition and lane change prediction on the highway." *2019 IEEE Intelligent Vehicles Symposium (IV)*. IEEE, 2019.

[11] Wang, Weida, et al. "An intelligent lane-changing behavior prediction and decision-making strategy for an autonomous vehicle." *IEEE Transactions on Industrial Electronics* 69.3 (2021): 2927-2937.

[12] Tang, Jinjun, et al. "A hierarchical prediction model for lane-changes based on combination of fuzzy C-means and adaptive neural network." *Expert systems with applications* 130 (2019): 265-275.

[13] Xia, Yingji, et al. "A human-like model to understand surrounding vehicles' lane changing intentions for autonomous driving." *IEEE Transactions on Vehicular Technology* 70.5 (2021): 4178-4189.

[14] Chu, Keonyup, Minchae Lee, and Myoungho Sunwoo. "Local path planning for off-road autonomous driving with avoidance of static obstacles." *IEEE transactions on intelligent transportation systems* 13.4 (2012): 1599-1616.

[15] Wang, Hongling, Joseph Kearney, and Kendall Atkinson. "Robust and efficient computation of the closest point on a spline curve." *Proceedings of the 5th International Conference on Curves and Surfaces*. 2002.

[16] Simon, Dan. *Optimal state estimation: Kalman, H infinity, and nonlinear approaches*. John Wiley & Sons, 2006.

[17] Bar-Shalom, Yaakov, X. Rong Li, and Thiagalingam Kirubarajan. *Estimation with applications to tracking and navigation: theory algorithms and software*. John Wiley & Sons, 2004.

[18] Gao, Bingbing, et al. "Interacting multiple model estimation-based adaptive robust unscented Kalman filter." *International Journal of Control, Automation and Systems* 15.5 (2017): 2013-2025.

[19] Krajewski, Robert, et al. "The highd dataset: A drone dataset of naturalistic vehicle trajectories on german highways for validation of highly automated driving systems." *2018 21st International Conference on Intelligent Transportation Systems (ITSC)*. IEEE, 2018.